Received: 11 August 2023 | Revised: 2 July 2024 | Accepted: 13 August 2024

DOI: 10.1111/mec.17512

ORIGINAL ARTICLE

MOLECULAR ECOLOGY WILEY

36-year study reveals stability of a wild wheat population across microhabitats

Tal Dahan-Meir[1,2] | Thomas James Ellis[2] | Fabrizio Mafessoni[1] | Hanan Sela[3,4] | Ori Rudich[1] | Jacob Manisterski[4] | Naomi Avivi-Ragolsky[1] | Amir Raz[1,5] | Moshe Feldman[1] | Yehoshua Anikster[4,#] | Magnus Nordborg[2] | Avraham A. Levy[1]

[1]Department of Plant and Environmental Sciences, Weizmann Institute of Science, Rehovot, Israel

[2]Gregor Mendel Institute, Austrian Academy of Sciences, Vienna BioCenter, Vienna, Austria

[3]Institute of Evolution, University of Haifa, Haifa, Israel

[4]The Institute for Cereal Crops Improvement, Tel-Aviv University, Tel Aviv, Israel

[5]Migal, Galilee Technology Center, Kiryat Shmona, Israel

Correspondence
Avraham A. Levy, Department of Plant and Environmental Sciences, Weizmann Institute of Science, Rehovot, Israel.
Email: avi.levy@weizmann.ac.il

Magnus Nordborg, Gregor Mendel Institute, Austrian Academy of Sciences, Vienna BioCenter, Vienna, Austria.
Email: magnus.nordborg@gmi.oeaw.ac.at

Funding information
SAERI; European Molecular Biology Organization, Grant/Award Number: STF 8368; Yeda-Sela Center

Handling Editor: Ana Caicedo

Abstract

Long-term genetic studies of wild populations are very scarce, but are essential for connecting ecological and population genetics models, and for understanding the dynamics of biodiversity. We present a study of a wild wheat population sampled over a 36-year period at high spatial resolution. We genotyped 832 individuals from regular sampling along transects during the course of the experiment. Genotypes were clustered into ecological microhabitats over scales of tens of metres, and this clustering was remarkably stable over the 36 generations of the study. Simulations show that it is difficult to determine whether this spatial and temporal stability reflects extremely limited dispersal or fine-scale local adaptation to ecological parameters. Using a common-garden experiment, we showed that the genotypes found in distinct microhabitats differ phenotypically. Our results provide a rare insight into the population genetics of a natural population over a long monitoring period.

KEYWORDS
adaptation, conservation genetics, population dynamics, population ecology, wheat, wild populations

1 | INTRODUCTION

The spatial and temporal scale of population genetic dynamics are key to understanding questions of adaptation and the response to selection. For example, how does the scale of genetic variation correspond to that of environmental variation, and how quickly can populations respond to natural selection? To address these questions, we need to describe the spatial structure of genetic variation, and track how this changes over many generations.

Previous studies of plant wild populations have included fine spatial collections (Hendrick et al., 2016; Li, Fahima, Peng, et al., 2000; Schemske, 1984; Todesco et al., 2020; Volis

#Deceased.

et al., 2004, 2015, 2016). Numerous studies have examined the spatio-temporal dynamics of wild plant populations over multiple years (Frachon et al., 2017; Franks et al., 2007; Fu et al., 2019; Horovitz & Feldman, 1991; Kelly, 2022; Kolis et al., 2022; Monnahan & Kelly, 2017; Ozbek et al., 2007; Troth et al., 2018), while a few studies have examined the temporal scale of allele frequency change over decades, especially in long-lived vertebrates (Aguillon et al., 2017; Ashraf et al., 2021; Chen et al., 2019; Stoffel et al., 2021). However, there are essentially no genetic studies examining both spatial and temporal dynamics of wild plants' populations over decades.

We examined the genetic diversity of a population of wild emmer wheat (*Triticum turgidum ssp. dicoccoides*) in Ammiad, Israel, which has been monitored for 36 years (Figure 1). Wild emmer wheat is an annual, self-pollinating, allotetraploid cereal (genome BBAA). It is the progenitor of durum wheat (*T. turgidum ssp. durum*) and the maternal donor of the A and B sub-genomes of bread wheat (*T. aestivum*, genome BBAADD) (Levy & Feldman, 2022). Its biodiversity is an invaluable resource for food security, due to the fact that major effect loci from wild emmer wheat could potentially be transferred to the background of domesticated wheat. The Ammiad population shows high genetic diversity compared to other wild wheat populations (Felsenburg et al., 1991; Levy & Feldman, 1988), together with variable topography (Figure 1, Movie S1) and a diversity of ecological niches within the scale of tens of metres (Anikster & Noy-Meir, 1991; Noy-Meir, Agami, Cohen, et al., 1991). The site is within a protected nature reserve, allowing repeated sampling of the population along transects that encompass considerable environmental variation. In this study we genotyped samples from nine harvests of these transects between 1984 and 2020, which allowed us to characterise the spatial and temporal dynamics of genetic change at Ammiad. Earlier works suggesting that plants in Ammiad are adapted to microhabitats (Anikster et al., 1991; Li, Fahima, Krugman, et al., 2000; Noy-Meir, Agami, Cohen, et al., 1991) were later disputed by Volis (Volis et al., 2015, 2016). Our dataset provides an almost unique insight into genetic change in a natural population of a predominantly selfing plant over time and space.

This is especially relevant, because wild progenitors of modern crops such as wild emmer wheat serve as an immense reservoir of biotic and abiotic stress-resistance genes (Khoury et al., 2021) that could be utilised to improve commercial varieties. Sustained studies of progenitor species in their natural ecological niches can provide a better understanding of their survival in different ecological niches, and inform strategies for conservation of such resources in situ, as well as in gene banks (Wintle et al., 2019).

Here, we describe patterns of genetic variation at Ammiad in time and space. We then investigate whether an apparent association with microhabitat might be biologically meaningful by comparing the observed pattern of variation to an explicit model accounting for the limited seed and pollen dispersal of a predominantly self-fertilising

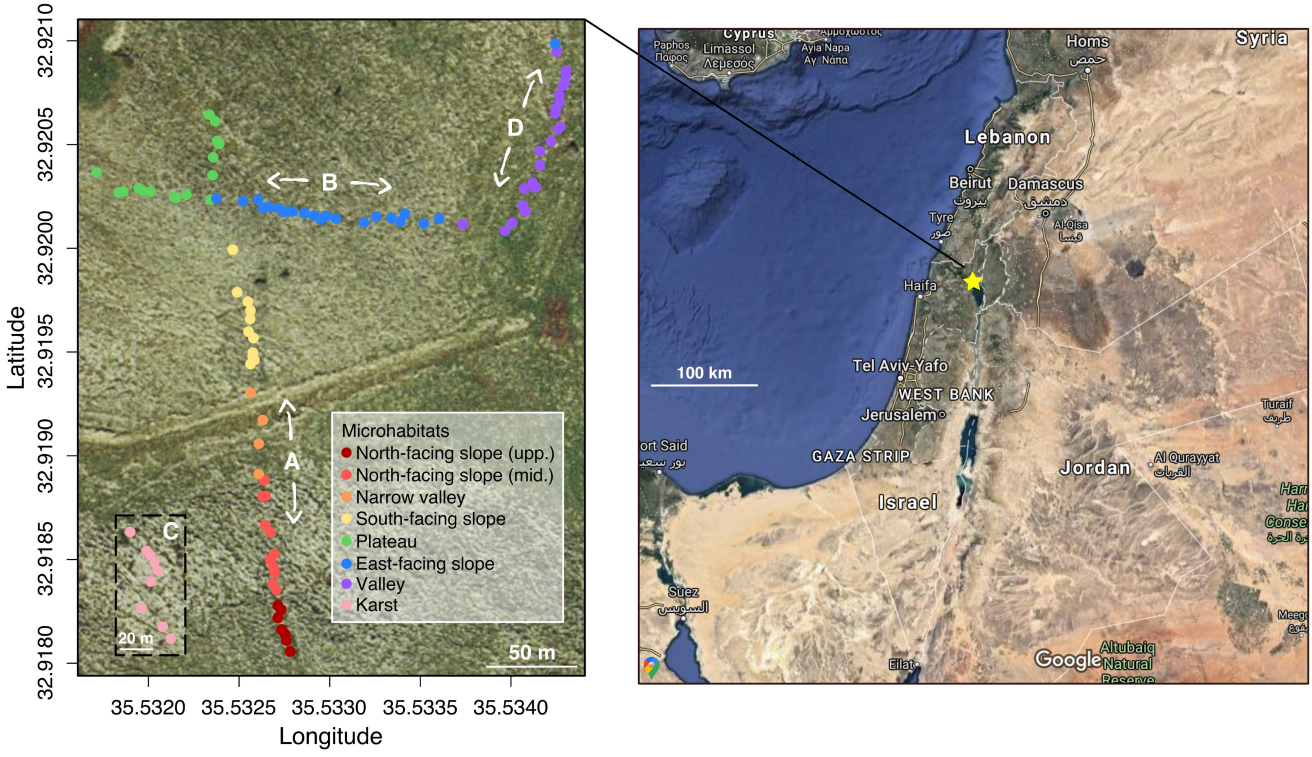

FIGURE 1 Ammiad wild-wheat population study. Location of Ammiad near the lake of Galilee (star, right and geographical coordinates, left). Sampling points of transects A–D collected in the years 1984, 1988, 1992, 1996, 2002, 2014, 2016, 2018 and 2020. Sampling points are shown on-site for transects A, B and D, but transect C, shown in the dashed rectangle, is located ~500 m north-west of A, B and D. Colours correspond to the different microhabitats labelled in the legend. The map on the left is taken from gov.map.co.il, and the map on the right is taken from Google Maps.

plant. Additionally, we tested whether the genetic clustering corresponds with phenotypes using a common-garden experiment. Finally, we discuss the implications of these results for local adaptation and conservation.

2 | RESULTS

2.1 | The population is composed of groups of near-identical genotypes

We catalogued the genetic diversity at Ammiad by repeated sampling over 36 years. We marked 100 sampling locations with pegs and recorded GPS coordinates along four transects traversing seven ecologically distinct microhabitats (Anikster & Noy-Meir, 1991; Figure 1, Dataset S1, Movie S1, Table S1). We sampled seeds from the closest plant to each sampling location at each of nine time points, and sowed them in the greenhouse for genotyping. In total, we genotyped 832 individuals using a genotyping-by-sequencing (GBS) protocol (Poland et al., 2012), resulting in 5196 single copy, single nucleotide polymorphism (SNP) markers that were unambiguously positioned on the wild emmer wheat reference genome (Avni et al., 2017).

As expected for a highly selfing species (The 1001 Genomes Consortium, 2016), the population is almost entirely composed of genetically distinct groups of nearly identical, highly homozygous individuals, clustered in space. Pairwise genetic identity follows a multimodal distribution that is characterised by pairs of plants that are either effectively identical, or share 70%–90% of SNP alleles (Figure 2). We unambiguously assigned all individuals to distinct genotype groups (DGGs) using a cut-off of >98% allele-sharing. This resulted in 118 DGGs over all nine time points, including 61 singletons (DGGs with a single member). The 10 largest DGGs encompass 65% of the samples, while the number of DGGs per year varied between 32 in 2014 and 49 in 1988 (Dataset S1). Rarefaction curves indicate that the sampling scheme was sufficient to detect almost all of the DGGs present close to the transects (Figure S1).

We also identified 15 (1.8%) highly heterozygous plants, which is consistent with outcrossing in recent ancestors. Using SNPMatch (Pisupati et al., 2017), we were able to identify the parental DGGs of two of these heterozygous individuals (Figure S2), suggesting that outcrossing happens between plants that are nearby. We estimated an average outcrossing rate of 3.7% across years in Ammiad, with detectable variation between the different habitats (1.8%–8.8%, Table S2). These values are compatible with estimates in bread wheat (*Triticum aestivum*) (Enjalbert & David, 2000).

2.2 | Genotypes are clustered by microhabitats and are stable through time

The spatio-temporal distribution of DGGs indicates two clear patterns (Figure 3). First, DGGs tend to cluster in space, as can be seen by the clustering of points of the same colour in Figure 3, and as would be expected for a self-compatible organism with limited dispersal. However, the clustering (Figure 3) and a principal component analysis of molecular variation (Figure S3a,b) show a striking concordance with the boundaries of ecological microhabitats, which were defined by Noy-Meir, Agami, Cohen, et al. (1991) based on topographic and floristic data without knowledge of the genetic structure of the population (Noy-Meir, Agami, Cohen, et al., 1991; Figure 3). For example, in transect A, there is a sharp transition between DGGs between the upper and middle north-facing slopes across the 36 years of study (Figure 3a). Another example is the genotype at collection point A59 in a unique location under the shade of a *Ziziphus spina-christi* tree (Figure 3a, south-facing slope). In contrast, in transect D, where there is negligible microhabitat differentiation, there is little spatial clustering of DGGs (Figure 3d). Population differentiation measured by F_{st} was consistently higher between microhabitats than within, even when taking distance into account (Figure 4a,b), and genetic distances are strongly correlated with microhabitats (Table S3, Figure S4). We also found greater differentiation among DGGs between microhabitats than would be expected by chance with the same level of spatial autocorrelation using a test based on Moran-spectral-randomisation Mantel statistics (MSR-Mantel) that explicitly account for spatial distance (Figure S5). In summary, DGGs are associated with ecological microhabitats at the scale of tens of metres.

Second, the spatial clustering of DGGs was stable through time, as seen by the vertical bands of identical colours in Figure 3. For example, 33% of plants sampled in 1984 belonged to the same DGG as plants sampled at the same position in 2020. An analysis of molecular variance (AMOVA) showed that 28% of the genetic variation between samples is explained by differences between microhabitats, and that the habitat effect is highly significant (Table S4). Conversely, time did not explain a significant proportion of variance (variance explained <1%), suggesting a strong stability of the genetic structure over time (Table S4). These results suggest that space, and particularly microhabitats, might constrain the genetic structure of Ammiad to be stable over the scale of tens of generations.

2.3 | Very low outcrossing rates may explain spatial differentiation

Our findings indicate that the genetic structure at Ammiad is more clustered into environmental microhabitats than would be expected under a null hypothesis of no clustering. However, it is clear that such a strict null hypothesis is not a good reference because it ignores the underlying biology of pollen and seed dispersal. To generate a more biologically realistic alternative hypothesis we tested whether the patterns at Ammiad can be explained using explicit demographic models that incorporate self-fertilisation and limited dispersal. The question is whether these neutral demographic processes – on their own – could maintain the spatial clustering into microhabitats observed at Ammiad.

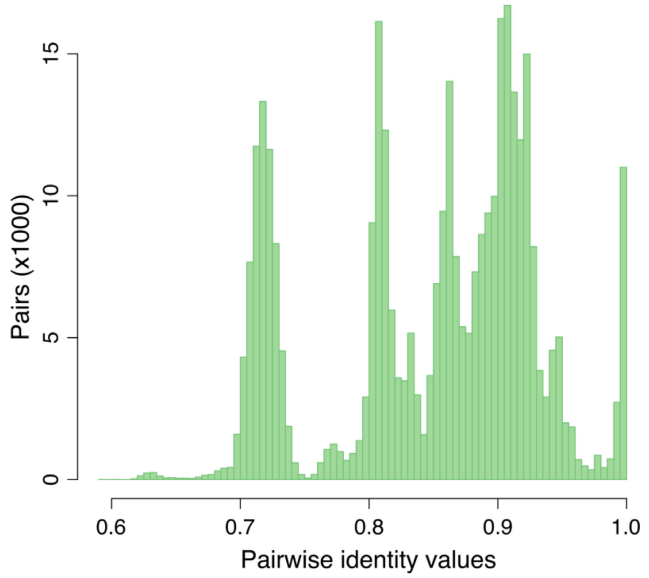

FIGURE 2 Distribution of pairwise identity values between the plants in Ammiad collection.

We performed individual-based simulations of populations of plants that initially reflect the genetic structure at Ammiad, and subsequently evolve by seed dispersal and outcrossing only (see *Materials and Methods*). We aimed to parameterise simulations using values for seed dispersal, plant density, outcrossing rate and seed dormancy that span the range of biologically realistic values. Individuals exist in a continuous two-dimensional habitat, but are sampled along linear transects in the same way as the real population. In this way we aimed to simulate a population evolving in the absence of selection and to sample it in a way that mimics the sampling of the study site at Ammiad.

We compared the change in genetic differentiation among microhabitats in observed and simulated populations by tracking the change in F_{st} through time (Figure 5). At Ammiad F_{st} fluctuated between 0.08 in 1988 and 0.26 in 1996, but remained stable at around 0.15 on average throughout the period of study. When outcrossing rates in simulations were at their lowest value (0.5% per generation) F_{st} was similarly stable across time (Figure 5, top row). For all other parameter combinations we observed a steady decrease in F_{st} in simulated populations over the 40 generations. The rate of decay was markedly faster as outcrossing rates increased, and depended surprisingly little on dispersal distance, seed dormancy or plant density. We also simulated values with mean dispersal of 0.1 m, but in these simulations individuals remained clustered close to the maternal plant, meaning that the population was so sparse that hardly any plants were close enough to transect sampling points to be sampled. Together, these results indicate that very low outcrossing rates could maintain the spatial clustering of genotypes found at Ammiad, but that limited outcrossing of a few percent combined should be sufficient to erase any apparent sorting into microhabitats within the period of study examined here.

2.4 | Phenotypes measured in a common garden predict phenotypic differentiation between habitats

We investigated whether genetic spatial differentiation is mirrored by differences in phenotypes. Owing to the challenging terrain and the status of the site as a protected conservation area it is not possible to estimate phenotypes with replication in a common-garden experiment under field conditions. We instead sowed six replicates of 92 DGGs (See *Materials and Methods*) in fully randomised blocks (Dataset S2) and measured 13 phenotypes related to growth and reproduction (Figure S6) in a controlled net house experiment that aimed to mimic conditions at Ammiad as closely as possible (see *Materials and Methods*). We first estimated broad-sense heritabilities for these traits, reflecting the proportion of variation in phenotypes explained by DGGs. With the exceptions of germination date, number of spikes and number of tillers, broad-sense heritabilities (on the scale of the link functions; de Villemereuil et al., 2016) were moderate to high (Figure 6a), indicating that substantial genetic variation exists for these traits.

We then used phenotype estimates from the net house to predict phenotypic differentiation in the field. A linear discriminant analysis that accounts for all traits jointly revealed clear clustering by microhabitat, with seed traits explaining the most separation (Figure S7; Table S5). For each trait separately, we then calculated the variance in each trait explained by habitat and year. For the three traits that showed low heritability (tiller number, spikelet number and germination time; Figure 6b) differences in habitat explained a very small proportion of phenotypic variation. For other traits, differences between habitats explained 19%–33% of the phenotypic variation for all traits (based on posterior means; Figure 6b), whereas variation between years explained <10% of the overall phenotypic variance in the population. There thus seems to be differentiation in heritable traits between habitats which remains stable through time, consistent with the spatial and temporal patterns observed among DGGs.

We next asked whether spatial structure in phenotypes corresponds to the structure of microhabitats. We compared the predicted phenotypes to a 'rotated' dataset where the vector of phenotypes is offset by a random number of positions relative to the vector of habitat labels. This preserves the structure of phenotypes and habitat labels, but breaks any covariation between phenotype and habitat. In rotated datasets habitat typically explained less than 20% of the variation in phenotype. This is similar to that explained by the three predicted phenotypes with low heritability, but less than that explained by the 11 remaining phenotypes for more than 99% of predicted datasets (Figure 6b). Our results indicate that the genetic clustering by microhabitat is matched by phenotypic differentiation between microhabitats.

3 | DISCUSSION

Studies of natural populations rarely have fine-scale geographical resolution or temporal resolution beyond the duration of a PhD or

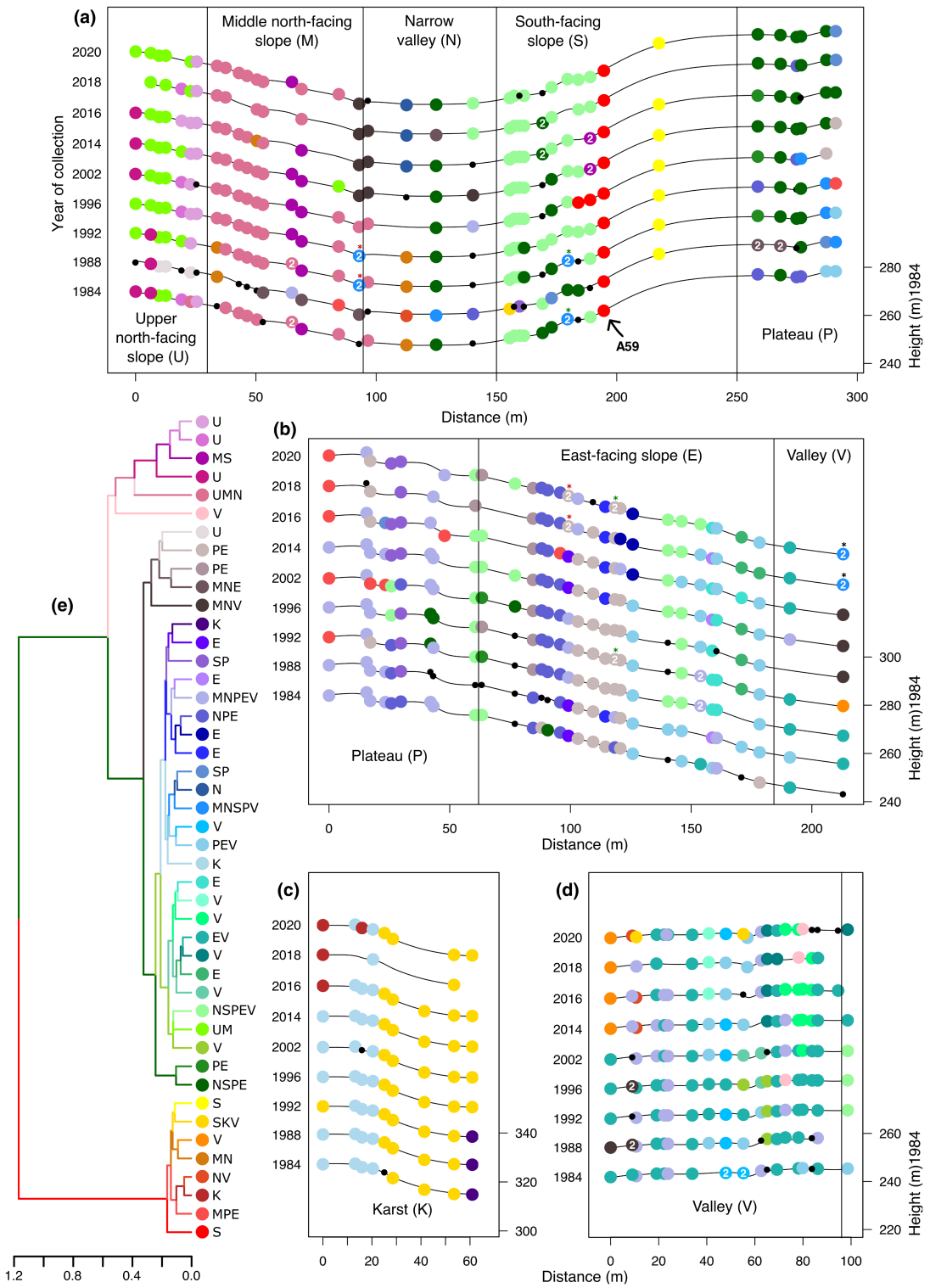

FIGURE 3 Spatio-temporal distribution of genotypes. (a–d) Distribution of samples coloured by distinct genotype group (DGG) in transects A–D. Y-axes indicate year of collection (left) and altitude for 1984 (right). Singleton samples are marked in small black dots, while doubleton groups are marked with '2' in the middle with the colour of their closest DGG. Doubleton groups that are closest to the same DGG were marked with coloured asterisks. DGGs with three or more samples are coloured in a unique colour. (e) Dendrogram of DGGs with three or more samples, hierarchically clustered by UPGMA. Labels at the tips of the dendrogram indicate all microhabitats in which each DGG is found.

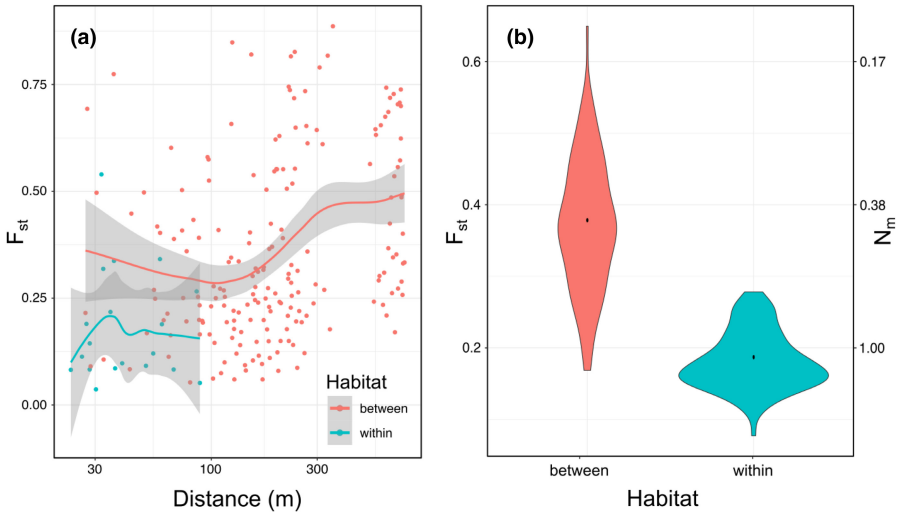

FIGURE 4 Spatial clustering at Ammiad. Genetic differentiation between and within habitats. To test whether population differentiation is higher when measured between plants occurring in different microhabitats than within the same microhabitat at random, we grouped plants into demes of 30 m. (a) Pairwise F_{st} among demes within and between habitats as a function of distance, measured as the average distance of plants in the two demes. Credibility intervals of a loess fit with degree 1 are shown in grey. N_m values (i.e. the theoretical number of migrants between demes in an infinite island model) calculated are shown on the right axis. (b) Pairwise F_{st} demes within and between habitats with average distance <50 m between each other. Average observed values are shown as a black dot. Uncertainty was estimated with 1000 bootstraps of the demes considered for the comparisons. Average within-habitat F_{st} was higher than between-habitat F_{st} in 3% of the bootstraps. N_m values (i.e. the theoretical number of migrants between demes in an infinite island model) calculated are shown on the right axis.

postdoc (Siepielski et al., 2009). Our study, spanning over 36 years of dense sampling, has both, and thus provides a unique dataset that could improve our understanding of gene flow and local adaptation on an ecological scale.

We found strong spatial clustering of genotypes that is stable through time and associated with ecological microhabitats. One explanation for this observation is that this clustering arises as a by-product of neutral demographic processes (Volis et al., 2015, 2016), and that the association with microhabitats is coincidence. An alternative explanation is that the stable spatial clustering of genotypes is due to a combination of neutral processes and fine-scale local adaptation to specific microhabitats. Since wild emmer wheat is a self-fertile organism with limited seed dispersal it is inevitable that spatial structure is at least partially driven by neutral processes, but two lines of evidence suggest a role for selection as well. First, in our simulations we found that only very low outcrossing rates could maintain the structure in the absence of selection, and that outcrossing of a few percent should be sufficient to erase the structure within the period studied here. Golenberg (1988) estimated outcrossing rates to be sufficiently low to maintain this structure. However, this estimate is based on another population using a relatively small sample and few allozyme markers, so it is not clear that this estimate is applicable to our sample. Our estimates suggested much higher outcrossing rates of a magnitude that would make it very difficult to maintain the structure observed at Ammiad. Second, if there is selection for microhabitats and outcrossing is as high as our estimates indicate, we would also expect to see phenotypic differentiation between microhabitats. Consistent with this we found that predicted phenotypes were more strongly associated with microhabitat than would be expected by chance. The association of genotypes and phenotypes with microhabitats and the difficulty of maintaining this structure in the face of substantial outcrossing, are evidence for the contribution of local adaptation to fine-scale population structure in this wild emmer wheat population.

The robustness of this result relies heavily on how realistic our simulations are at capturing the true population dynamics. The parameter values used for the means of the four variables modelled were motivated by empirical data, and we are confident that these span and go beyond biologically realistic values. Nevertheless, it may be that our simulations do not sufficiently capture the variance around these means. For example, we modelled fecundity and dispersal as being exponentially distributed, but in plant populations these variables are frequently overdispersed relative to an exponential (Clark, 1998; Clark & Ji, 1995). Likewise, we modelled plant density as constant in time and space, whereas in reality density fluctuates across both. The increased variance in fecundity, dispersal and density caused by these phenomena may inflate the importance of neutral processes in maintaining the genetic and phenotypic structure of the population Ammiad in a way that is not captured by our simulations. Although it is fairly straightforward to define a model that allows for the variance due to these phenomena (e.g. dispersal is often modelled as a generalised normal distribution; Austerlitz et al., 2004), we did not attempt to do so because we lack suitable empirical data to parameterise such models. We speculate that our results are likely still valid because we consider mean parameter values that are beyond the lowest range of empirical estimates. Nevertheless, we cannot exclude that the spatio-temporal

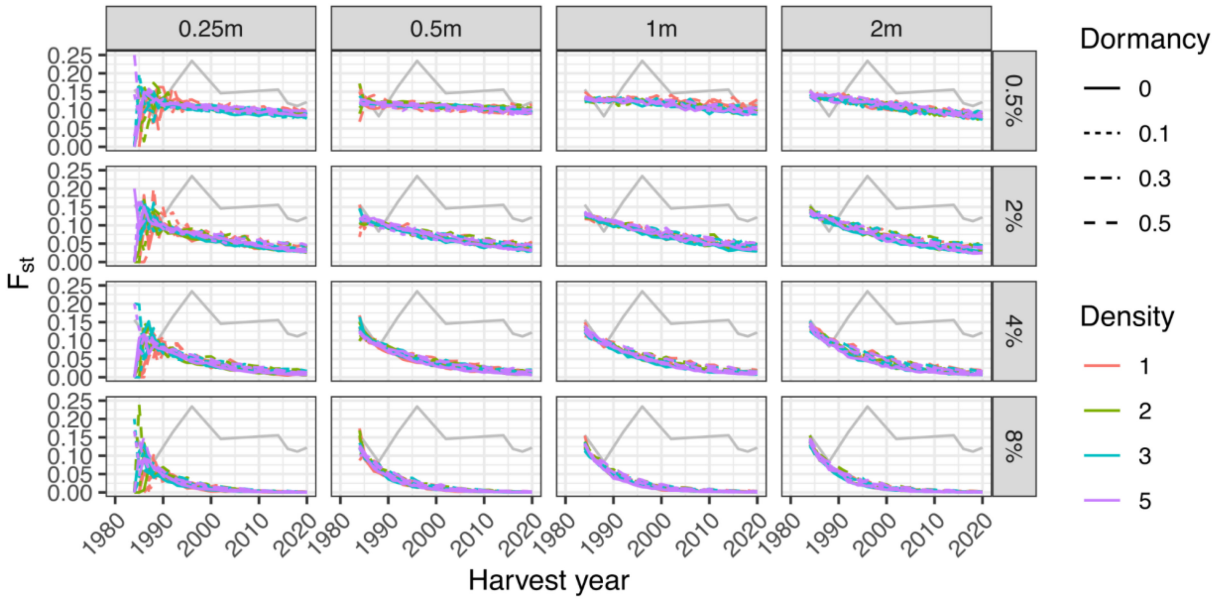

FIGURE 5 Genetic differentiation between microhabitats at Ammiad and in simulated populations. Grey lines show F_{st} between microhabitats across all transects at Ammiad. Coloured lines show average F_{st} over 100 replicate simulations that begin with the genetic structure at Ammiad in 1984 but evolve neutrally after that. Curves indicate different combinations of mean dispersal distance (grey boxes, panels left to right), outcrossing rate (grey boxes, panels top to bottom), proportion of seeds coming from the seed bank (dashed lines) and plant density per square metre (colours). For clarity, the y-axis has been clipped at 0.25.

patterns at Ammiad are due to rare stochastic events that were not modelled in our simulations.

In summary, although there is evidence for local adaptation to microhabitats in maintaining the genetic structure at Ammiad, this dataset does not allow us to categorically reject the null hypothesis that variation is strictly neutral. Ideally, reciprocal transplant experiments between microhabitats in the field would be necessary to properly demonstrate that variation is adaptive. However, this is not feasible owing to the challenging terrain, and the status of the Ammiad site as a nature reserve. This issue highlights the complexity of accounting for historical demography to properly define competing biological hypotheses.

Although climate change was not yet an established fact in 1984, it became part of the motivation of Ammiad experiment. In retrospect, the increase in local ambient temperatures by ~1.5 degrees Celsius (Figure S8a) and in atmospheric CO_2 concentration by 70 ppm (Figure S8b, Keeling et al., 2001) during the course of the experiment, could have led to selection that affected the population structure. However, only minor temporal changes were seen. This genetic temporal stability could be interpreted as the population not having had enough time to adapt due to the rapid pace of climatic changes, in which case we would expect a reduction in fitness of the population. However, plant density was similar in 1984 and in 2020, suggesting that, so far, this has not occurred. Wild emmer wheat might have evolved to be resilient to temperature fluctuations since its speciation 0.8 MYA ago (Levy & Feldman, 2022) and that recent climate changes might not have yet reached the threshold that endangers the species.

Our results are relevant to conservation strategies as well as to the assessment of biodiversity resilience under climate change. First, our study shows that in-situ conservation can be quite effective in preserving diversity, without the need to frequently sample seeds and store them in seed banks (ex-situ). Second, our results highlight that effective in-situ and ex-situ conservation strategies of wild plants biodiversity, particularly for wild grasses and crop progenitors such as wild emmer wheat, should consider habitat diversity as a potential reservoir of adaptive diversity. In fact, our long-term study would not have been possible if the site had not been declared a natural reserve for wild-wheat conservation by the Israel nature and parks authority. Indeed, this population is fenced and undergoes moderate grazing. Unrestricted grazing, or urbanisation, as seen in other parts of the Levant can reduce and sometimes eliminate wild grasses. The Ammiad reserve is relatively small (~10 hectares) but contains much diversity. Establishing natural reserves of crop progenitors, partially protected from anthropogenic activities, does not necessarily require large areas and is a feasible goal that is critical for biodiversity conservation.

In conclusion, we provide a unique example of strong temporal stability, a counterpoint to recent studies demonstrating dramatic changes in local populations even between seasons (Bergland et al., 2014; Machado et al., 2021; Rudman et al., 2022; Wittmann et al., 2017). Fully explaining this stability will require further work, but, whatever the causes, such robustness in a rapidly changing world demonstrates the importance of conservation of wild relatives of crops in nature, as gene pools for breeding (Zsögön et al., 2021).

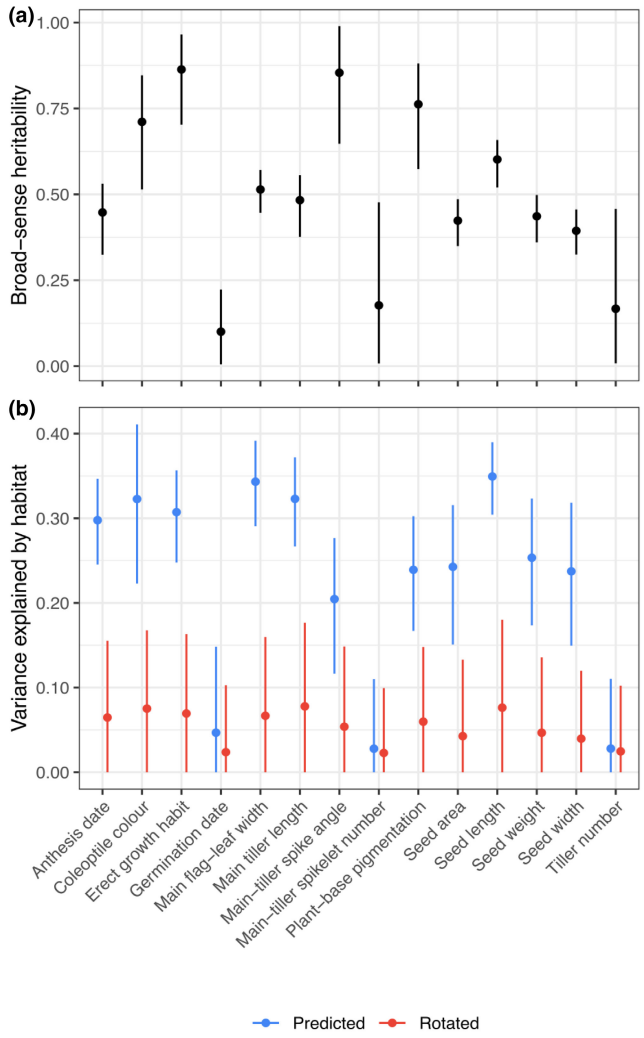

FIGURE 6 Heritability and variance explained by habitat for in predicted phenotypes at Ammiad. (a) Posterior mean and 95% credible intervals for broad-sense heritability of 14 phenotypic traits measured on six replicates each of 95 homozygous DGGs in a common-garden net house experiment. Because traits display a range of error distributions, heritability is calculated on the scale of the corresponding link functions for comparison. (b) Plots show the posterior mean and 95% credible intervals for 801 field samples predicted (blue) from traits measured in the net house experiment. Variance components are shown for the raw predictions based on real microhabitat positions, and for 'rotated' data (red) where microhabitat labels were offset by a random number of positions to break any correlation between phenotypic traits and microhabitats.

4 | MATERIALS AND METHODS

4.1 | Sample collection and DNA extraction

Wild wheat spikes were collected in four different linear transects every 3–5 m from sampling points marked with pegs and GPS coordinates (Dataset S1). Plants were assigned to a sampling point when collected in successive years in a radius of ~1 m from the peg. We propagated seeds from all field samples in a nethouse in the year following collection. For samples from 2014 to 2022 we collected tissue directly from these progeny. For samples from 1984 to 2002 we propagated a second generation of seeds in 2015 and collected tissue from these plants. Tissue was ground using mortar and pestle with the addition of Merck sea-sand in liquid nitrogen. DNA extraction was done using Macherey-Nagel NucleoSpin® Plant II extraction kit, according to the manufacturer's protocol, eluting in 50 μL EB total. Concentrations and DNA quality were estimated using a NanoDrop® ND-1000 Spectrophotometer.

4.2 | Genotyping by sequencing and variant calling

Plant genotyping was done according to the GBS method (Elshire et al., 2011; Poland et al., 2012), using *MspI* and *PstI-HF* restriction enzyme, and 96 barcodes of plate 384A (Poland et al., 2012). Samples were sequenced using Illumina NextSeq 550 mid-output 150 base-pairs single-end kits. A reference sample, Zavitan accession (Avni et al., 2017), was added to each run, undergoing the same plate GBS library preparation and sequencing. Samples were divided by barcodes using a python 2.7 code. The mean and median number of raw FASTQ reads were 2,270,374 and 1,989,792 respectively. Mapping to the WEW_v2.0 genome assembly (Zhu et al., 2019) was done using *bwa-mem* (Li, 2013). Conversion to binary alignment map (BAM) format, filtering for uniquely mapped reads with minimum QUAL score of 30, sorting and indexing was done using SAMtools (Li et al., 2009). The mean and median number of reads mapped and filtered were 1,026,255 and 908,202, respectively. Variant calling was done in parallel running on all 845 (832 Ammiad samples and 13 Zavitan controls) samples using GATK HaplotypeCaller 3.8 (Poplin et al., 2018), resulting in 3,077,682 SNP markers. Filtering for quality (>30), read depth (>6), genotype quality (>15), maximum missing sites (10%) and no-indels was done using VCFtools (Danecek et al., 2011), resulting in 5995 SNP markers. Heterozygous SNPs in >10% of the accessions were filtered out from the analysis using TASSEL5 (Bradbury et al., 2007). Filtered VCF, consisting of 5196 SNP markers, was used for all further analyses (see *Data availability statement*).

4.3 | Pairwise genetic identity

We measured genetic identity using R (see *Data availability statement*) by calculating the pairwise identity values between all samples, divided by the number of comparisons. The pipeline also divides the samples into DGGs by setting a threshold of 98.1% identity of the variant sites, which is the lowest threshold where no sample is assigned to two or more DGGs, and constructs the dendrogram describing the relatedness between the DGGs. We performed hierarchical clustering R by UPGMA (method "average" in *hclust* function). All samples of the reference accession, Zavitan, were grouped together into one DGG, indicating that we can reliably group identical genotypes.

4.4 | Rarefaction and principal component analyses

In order to test whether the samplings of Ammiad populations were sufficient to detect the majority of DGGs, we performed rarefaction analyses using R (see *Data availability statement*) by taking successively small subsamples of the DGGs present in each year, and fitting a polynomial curve to the number of unique DGGs sampled across subsamples. We repeated this 100 times for each year.

We performed principal component analysis on the VCF file of the entire Ammiad collection using *SNPRelate* R Package (Zheng et al., 2012). We calculated identity by distance for each transect separately.

4.5 | Outcrossing estimation and parental lines detection

To estimate outcrossing we calculated F_{IS} using the R package *hierfstat* (Goudet, 2005). We calculated confidence intervals as the 2.5% and 97.5% quantiles of 100 bootstraps using the function boot.ppfis. We estimated outcrossing rates (f) using the relationship $F_{IS}=(1-f)/(1+f)$ (Wright, 1969). To detect the parental DGGs of heterozygous plants we used SNPMatch (Pisupati et al., 2017) by comparing each plant to a database of all DGGs.

4.6 | Microhabitat clustering analysis

We tested whether population differentiation, measured by F_{st}, is higher when measured between plants occurring in different microhabitats than in the same microhabitat. To this goal we subdivided plants into demes with a maximum distance between plants of 30 m. We then computed the pairwise F_{st} between demes using the R package *pegas* (Paradis, 2010). To correct for the effects of isolation by distance and spatial structure we stratified comparisons by distance, measured as the distance between the average locations of plants in the two demes.

To account for spatial autocorrelation we first performed a partial Mantel test using the function *multi.mantel* from the R package *phytools* (Revell, 2012). Specifically, we considered as a response variable the pairwise genetic distances used to define DGGs. We tested for the effect of habitat, represented as a distance matrix with value '0' for plants found in the same microhabitat and '1' for plants found in two different microhabitats. In addition, we included in the test matrices of spatial and temporal distance. We estimated spatial distances based on latitude and longitude using the function *earth.dist* from the R package *fossil* (https://palaeo-electronica.org/2011_1/238/index.html). We detected a significant effect of space and microhabitat (p-values <.005 for both matrices) and a non-significant effect of time (p-value = .863).

Mantel and partial Mantel tests have been severely criticised for their inaccuracy in presence of high spatial autocorrelation (Crabot et al., 2019; Legendre et al., 2015). To account for these known biases, we used the approach proposed by (Crabot et al., 2019), which uses a Moran spectral randomisation procedure to generate random samples which maintain the same autocorrelation properties of the original dataset. To this goal, we used the R packages *sdpep* to process the spatial matrices and the *msr* function of the package *adespatial* (Guénard & Legendre, 2022). The distances above were transformed into Euclidean distances with function *cailliez* from the R package *adegenet* (Jombart & Ahmed, 2011). Using this approach, we tested the effect of habitat on both DGGs and pairwise genetic distances, using 1000 randomisations. In both cases the effect of microhabitat was significant (p-value <.05).

We computed an AMOVA using the R package *pegas* (Paradis, 2010), using plants sampled across all years. We included terms for microhabitat and year of collection (nested within microhabitat) in the model.

4.7 | Individual-based simulations

To investigate whether neutral demographic processes could maintain the degree of clustering observed at Ammiad in 1984 over the period of study we performed individual-based simulations of populations of plants evolving via seed dispersal and outcrossing only. An R package, *simmiad*, is provided to perform these simulations (DOI: https://zenodo.org/records/13364977).

We simulate populations of N plants evolving in a uniform square two-dimensional habitat with sides approximately twice the length of transect A, corresponding to the rough size of the Ammiad population. The simulated population begins with a structure that mimics that found at Ammiad with densities of 1, 2, 3 or 5 plants/m^2. One challenge is that the real population is sampled along a one-dimensional transect, but simulations need to be seeded in two dimensions. To do this we first concatenate the vector of genotypes from all transects in 1984, arrange them along sampling points 5 m apart along one axis of the habitat, then copied this structure in the perpendicular direction to create bands of identical genotypes in a grid. So as not to bias the measurement of the structure to any single region of the populations we 'rotated' the concatenated transect by a random number of positions in each simulation replicate. Sampling points are also assigned the same microhabitat label as they had at Ammiad, but we do not model selection for microhabitat. To ensure the population is at the correct density we then draw a sample with replacement of size N of plants on the grid to generate a population at generation 1. At 40 subsequent generations, N plants are sampled with replication to produce N seeds. We then draw a transect of 30 sampling points 5 m apart through the middle of the population at each generation, and sample the plant closest to each sampling point. This procedure replicates the continuous distribution of the plants, and the discrete procedure used to sample the population.

We ran simulations using different values of plant density, seed dormancy, outcrossing rate, and mean seed dispersal distance that span a range of biologically realistic values. Average plant density in the Ammiad population was measured in 1984 as 4 plants/m^2

(Noy-Meir, Agami, & Anikster, 1991). We repeated this measurement in 2020 for transect A and found a similar density of 3.8 plants/m^2 (Dataset S1). As such, we simulated values of plant density of 1, 2, 3 and 5 plants/m^2.This species has a substantial seed bank with up to 30% of germinating seedlings coming from the previous year, but very few from previous years (Horovitz, 1998), so from generation 3 onwards seeds are drawn from the previous generation with probability 1–*p*, and from two generations previous with probability *p*, for values of *p* of .5, .3, .1 or 0. Based on estimates of outcrossing rate by Golenberg (1988) of 0.5% and our estimates of up to 8% (Table S2), and are randomly assigned as outcrossed with probabilities 0.5%, 2%, 4%, or 8%. Since we have no information about pollen dispersal distance and are only concerned with tracking unique genotypes, outcrossed seeds are assigned a new unique genotype, just as outcrossed seeds in the real sample would appear as a unique DGG. Seed dispersal occurs through a combination of gravity, ants, birds, grazing mammals and rodents, enabling both short and long-distance dispersal. We lack direct estimates of seed dispersal distances, but average gene flow, a composite of seed and pollen dispersal, was estimated to be 1.25 m per year (Golenberg, 1987); since most dispersal is via seeds, the average seed dispersal distance is likely to be around 1 m per year. With this in mind, simulated offspring disperse from the mother in a random direction at a distance drawn from an exponential distribution with a mean of 0.25, 0.5, 1 or 2 m. To eliminate edge effects, the habitat is modelled as a torus, such that if dispersal takes a seed over the edge of the habitat it is reflected back to the opposite side.

We measure microhabitat differentiation on each sampled transect as

$$F_{st} = \left(f_0 - \underline{f}\right) / \left(1 - \underline{f}\right)$$

where f_0 is the is the probability that two individuals in the same subpopulation are the same DGG, and $\underline{f}$ is the probability that two individuals from the total population are the same DGG. For each combination of plant densities, outcrossing rates, seed bank parameter *p* and seed dispersal distances we performed 100 replicate simulations.

4.8 | Common-garden experiment

We established a common garden experiment in a net-house in the Weizmann Institute of Science. We grew plants from 92 distinct homozygous DGGs (seeds were taken from the single-seed propagations that were used for genotyping), including all 58 DGGs with two or more samples and 34 singleton DGGS, as well as the reference genotype 'Zavitan', in six fully randomised blocks in a net house (Dataset S2). To minimise effects caused by the different maternal growing environments of the original collections, we used seeds from the same plants that were used for genotyping that had been grown in a common environment. In order to keep conditions as similar as possible to the conditions in Ammiad site, we sowed seeds in mid-November in Terra Rossa soil collected at Ammiad. Plants were subject to natural winter rainfall, and we provided additional irrigation on two occasions when plants were close to desiccation.

We measured four phenotypes related to vegetative growth: (germination date; presence/absence of coleoptile anthocyanin pigmentation; erect growth habit, scored from 1 to 5; plant-base pigmentation during tillering, scored from 1 to 3), six phenotypes related to anthesis (anthesis date; main tiller length (cm) from the soil to the base of the spike; log main-tiller flag-leaf width (cm); main tiller number of spikelets; main tiller spike angle, scored from 1 to 3; number of tillers) After seed collection we measured four additional phenotypes based on 10 dry seeds per plant: seed area (mm^2), seed length (mm), seed width (mm) and the weight of 10 seeds (g) using VIBE QM3 seed analyser. Raw phenotypic data are provided in Dataset S2.

We estimated the posterior distribution of genetic values for each trait using a generalised linear mixed model in the R package *brms* (Bürkner, 2017). We model the phenotype z_{ijk} with link function $f(z)$ (with inverse function $f'(z)$) of a plant *i* of genotype *j* in block *k* as

$$z_{ijk} = f'\left(\eta_{ijk}\right)$$

where

$$\eta_{ijk} = \alpha + \gamma_j + \beta_k + \epsilon_i$$

α is an intercept, γ_j is the mean phenotype of DGG *j*, β_{km} is the mean phenotype for experimental block *k*, ϵ_i is a residual error term (for phenotypes with normally-distributed errors), and:

$$\alpha \sim t_3\left(\mu, \sigma_\alpha\right)$$

$$\gamma \sim t_3\left(0, \sigma_{\text{DGG}}\right)$$

$$\beta \sim t_3\left(0, \sigma_{\text{block}}\right)$$

where t_3 describes a *t*-distribution with 3 degrees of freedom. We used the default priors in *brms* for the mean and variance components. The 14 traits measured were a mixture of normally distributed, Poisson, binary and ordinal variables, so we used identity, log, logit and cumulative-logit link functions respectively, as appropriate. We standardised normally distributed traits by mean-centring and dividing by the standard deviation. We calculated broad-sense heritability on the scale of the link function following de Villemereuil et al. (2016) as

$$\frac{\sigma_{\text{DGG}}}{\sigma_{\text{DGG}} + \sigma_{\text{block}} + \sigma_\epsilon}$$

Note that for models with non-identity link functions σ_ϵ is only defined on the scale of the data, and does not contribute to heritability estimates on the scale of the link function (de Villemereuil et al., 2016; McCullagh & Nelder, 1989).

We used the linear models to predict phenotypic differentiation in the field. This is complicated by the fact that we expect DGGs to be partially, not completely, differentiated by microhabitat. That means that on one hand DGGs do not have a single

habitat of origin, but 'belong' to multiple microhabitats in different years. Moreover, replicates of the same DGG will be collinear with microhabitat. For these reasons it does not make sense to simply include a term for 'habitat' in the linear model. Instead, we use the nethouse data to predict phenotypes for the observed genotypes in the field, and calculate the variance in phenotypes explained by habitat on these predicted data. We drew 1000 values from the posterior distribution of each phenotype for each of the 832 samples in the field data set (excluding 117 empty sampling plots) using the *brms* function 'posterior_predict'. This function simulates phenotype values based on the genetic values for each DGG plus inter-individual error, accounting for uncertainty in both. For the 26 samples that were not included in the net-house experiment, we used *brms* to draw a phenotype value from the posterior distribution of genetic values of phenotyped DGGs. Since these values vary across posterior draws this allows us to assign phenotypes to the missing genotypes without biassing the distribution of phenotypes, and renders tests of association with microhabitat conservative.

We performed a linear discriminant analysis of the predicted phenotypes in the field as a function of microhabitat using the *MASS* library in R (Venables & Ripley, 2002). For this analysis we used posterior mean phenotypes for each DGG, using the 806 plants from DGGs that were included in the net-house experiment. We scaled numerical phenotypes by their standard deviations to ensure homogeneity of variance among phenotypes.

We then estimated the variance in each phenotype explained by habitat and year in each predicted dataset using *lme4* (Bates et al., 2015). To generate a null distribution for the association between phenotype and habitats we used a 'rotation' approach similar to that used to test sorting by microhabitat. We concatenated transects within each year into a single circular transect and 'rotated' the vector of predicted phenotypes by shifting each value a random number of positions. Values that are shifted beyond the length of the vector we reflected back from the beginning of the vector. This preserves spatial structure in phenotypes and microhabitats but breaks any association between them. We performed a single rotation for each of 1000 realisations of phenotype predictions. For each realisation we recalculated the variance in rotated phenotype explained by microhabitat and year, and compared the distribution of these variance estimates to those for the corresponding predicted dataset.

4.9 | Temperature and CO_2 concentration data

In order to demonstrate the climatic changes that took place during the course of Ammiad experiment, we obtained daily minimum and maximum temperatures data from 1984 to 2020 from Ayyelet Hashahar station from the Israeli Meteorological Service database at the Israel government portal (https://ims.gov.il/en/data_gov). We obtained data on weekly atmospheric CO_2 concentrations from The Scripps Institution of Oceanography UC San Diego (Keeling et al., 2001).

AUTHOR CONTRIBUTIONS

Tal Dahan-Meir, Moshe Feldman, Yehoshua Anikster and Avraham A. Levy conceived and designed the study. Tal Dahan-Meir carried out the molecular work, SNP calling, genetic and phenotypic analyses with input from Thomas James Ellis, Fabrizio Mafessoni, Magnus Nordborg and Avraham A. Levy. Thomas James Ellis performed the simulations and phenotypic analyses with input from Tal Dahan-Meir, Magnus Nordborg and Avraham A. Levy. Fabrizio Mafessoni carried out the population differentiation analysis, with input from Tal Dahan-Meir and Avraham A. Levy. Tal Dahan-Meir, Ori Rudich and Avraham A. Levy carried out the common-garden experiment. Tal Dahan-Meir, Hanan Sela, Jacob Manisterski, Naomi Avivi-Ragolsky, Amir Raz, Moshe Feldman, Yehoshua Anikster and Avraham A. Levy carried out the collection. Tal Dahan-Meir, Thomas James Ellis, Fabrizio Mafessoni, Magnus Nordborg and Avraham A. Levy wrote the manuscript. Magnus Nordborg and Avraham A. Levy supervised the project.

ACKNOWLEDGEMENTS

We thank T. Azulay, T. Grinevich, C. Melamed-Bessudo, O. Gross, R. Epstein, Z. Meir and members from the Institute for Cereal Crops Improvement at Tel-Aviv University for plant material collection. We thank A. Distelfeld and members of the Institute of Evolution, University of Haifa, for using their VIBE QM3 seed analyser, and J. Müller for the drone movie. We also thank N. Barkai, Y. Eshed, D. Filiault, K. Swarts, S. Nowoshilow, N. De-Malach, R. Pisupati, R. Burns, Y. Voichek, P. Clauw, E. Kosman and the Levy and Nordborg labs for fruitful discussions.

FUNDING INFORMATION

This work was supported by the Yeda-Sela Center and Sustainability and Alternative Energy Research Initiative (SAERI) of the Weizmann Institute of Science. T.D-M. acknowledges a European Molecular Biology Organization scientific exchange grant 8368.

CONFLICT OF INTEREST STATEMENT

The authors declare no competing interests.

DATA AVAILABILITY STATEMENT

Sequencing data generated in this study are available in the National Center for Biotechnology Information (NCBI) Sequence Read Archive (SRA) under the accession number PRJNA779576 (Dahan-Meir & Levy, 2022). All data processing and data analysis are publicly available on GitHub (https://github.com/TalDM/Ammiad) and Zenodo (https://doi.org/10.5281/zenodo.13364710) (Dahan-Meir et al., 2022). An R package, *simmiad*, is provided to perform the individual-based simulations (https://zenodo.org/records/13364977) (Ellis, 2022).

ORCID

Tal Dahan-Meir https://orcid.org/0000-0002-7876-4815

Thomas James Ellis https://orcid.org/0000-0002-8511-0254

REFERENCES

Aguillon, S. M., Fitzpatrick, J. W., Bowman, R., Schoech, S. J., Clark, A. G., Coop, G., & Chen, N. (2017). Deconstructing isolation-by-distance: The genomic consequences of limited dispersal. *PLoS Genetics*, *13*(8), e1006911.

Anikster, Y., Amram, E., Smadar, E., & Auguste, H. (1991). Patterns of phenotypic variation in wild tetraploid wheat at Ammiad. *Israel Journal of Botany*, *40*, 397–418.

Anikster, Y., & Noy-Meir, I. (1991). The wild-wheat field laboratory at Ammiad. *Israel Journal of Botany*, *40*, 351–362.

Ashraf, B., Hunter, D. C., Bérénos, C., Ellis, P. A., Johnston, S. E., Pilkington, J. G., Pemberton, J. M., & Slate, J. (2021). Genomic prediction in the wild: A case study in Soay sheep. *Molecular Ecology*, *31*, 6541–6555. https://doi.org/10.1111/MEC.16262

Austerlitz, F., Dick, C. W., Dutech, C., Klein, E. K., Oddou-Muratorio, S., Smouse, P. E., & Sork, V. L. (2004). Using genetic markers to estimate the pollen dispersal curve. *Molecular Ecology*, *13*(4), 937–954.

Avni, R., Nave, M., Barad, O., Baruch, K., Twardziok, S. O., Gundlach, H., Hale, I., Mascher, M., Spannagl, M., Wiebe, K., Jordan, K. W., Golan, G., Deek, J., Ben-Zvi, B., Ben-Zvi, G., Himmelbach, A., MacLachlan, R. P., Sharpe, A. G., Fritz, A., … Distelfeld, A. (2017). Wild emmer genome architecture and diversity elucidate wheat evolution and domestication. *Science*, *357*(6346), 93–97.

Bates, D., Mächler, M., Bolker, B. M., & Walker, S. C. (2015). Fitting linear mixed-effects models using lme4. *Journal of Statistical Software*, *67*(1), 1–48.

Bergland, A. O., Behrman, E. L., O'Brien, K. R., Schmidt, P. S., & Petrov, D. A. (2014). Genomic evidence of rapid and stable adaptive oscillations over seasonal time scales in drosophila. *PLoS Genetics*, *10*(11), e1004775.

Bradbury, P. J., Zhang, Z., Kroon, D. E., Casstevens, T. M., Ramdoss, Y., & Buckler, E. S. (2007). TASSEL: Software for association mapping of complex traits in diverse samples. *Bioinformatics*, *23*(19), 2633–2635.

Bürkner, P. C. (2017). brms: An R package for Bayesian multilevel models using Stan. *Journal of Statistical Software*, *80*, 1–28.

Chen, N., Juric, I., Cosgrove, E. J., Bowman, R., Fitzpatrick, J. W., Schoech, S. J., Clark, A. G., & Coop, G. (2019). Allele frequency dynamics in a pedigreed natural population. *Proceedings of the National Academy of Sciences of the United States of America*, *116*(6), 2158–2164.

Clark, J. S. (1998). Why trees migrate so fast: Confronting theory with dispersal biology and the paleorecord. *The American Naturalist*, *152*(2), 204–224.

Clark, J. S., & Ji, Y. (1995). Fecundity and dispersal in plant populations: Implications for structure and diversity. *The American Naturalist*, *146*(1), 72–111.

Crabot, J., Clappe, S., Dray, S., & Datry, T. (2019). Testing the mantel statistic with a spatially-constrained permutation procedure. *Methods in Ecology and Evolution/British Ecological Society*, *10*(4), 532–540.

Dahan-Meir, T., Ellis, T. J., & Mafessoni, F. (2022). *Ammiad scripts and analyses*. GitHub, Zenodo. https://github.com/TalDM/Ammiad, https://doi.org/10.5281/zenodo.13364710

Dahan-Meir, T., & Levy, A. A. (2022). *Ammiad wild wheat population samplings 1984–2020*. The National Center for Biotechnology Information (NCBI) Sequence Read Archive (SRA); PRJNA779576. https://www.ncbi.nlm.nih.gov/bioproject/PRJNA779576

Danecek, P., Auton, A., Abecasis, G., Albers, C. A., Banks, E., DePristo, M. A., Handsaker, R. E., Lunter, G., Marth, G. T., Sherry, S. T., McVean, G., Durbin, R., & 1000 Genomes Project Analysis Group. (2011). The variant call format and VCFtools. *Bioinformatics*, *27*(15), 2156–2158.

de Villemereuil, P., Schielzeth, H., Nakagawa, S., & Morrissey, M. (2016). General methods for evolutionary quantitative genetic inference from generalized mixed models. *Genetics*, *204*(3), 1281–1294.

Ellis, T. J. (2022). *Simmiad: An R package for individual-based simulations of the Ammiad population*. GitHub, Zenodo. https://github.com/ellisztamas/simmiad, https://zenodo.org/records/13364977

Elshire, R. J., Glaubitz, J. C., Sun, Q., Poland, J. A., Kawamoto, K., Buckler, E. S., & Mitchell, S. E. (2011). A robust, simple genotyping-by-sequencing (GBS) approach for high diversity species. *PLoS One*, *6*(5), e19379.

Enjalbert, J., & David, J. L. (2000). Inferring recent outcrossing rates using multilocus individual heterozygosity: Application to evolving wheat populations. *Genetics*, *156*(4), 1973–1982.

Felsenburg, T., Levy, A. A., Galili, G., & Feldman, M. (1991). Polymorphism of high-molecular-weight glutenins in wild tetraploid wheat: Spatial and temporal variation in a native site. *Israel Journal of Botany*, *40*, 451–479.

Frachon, L., Libourel, C., Villoutreix, R., Carrère, S., Glorieux, C., Huard-Chauveau, C., Navascués, M., Gay, L., Vitalis, R., Baron, E., Amsellem, L., Bouchez, O., Vidal, M., Le Corre, V., Roby, D., Bergelson, J., & Roux, F. (2017). Intermediate degrees of synergistic pleiotropy drive adaptive evolution in ecological time. *Nature Ecology & Evolution*, *1*(10), 1551–1561.

Franks, S. J., Sim, S., & Weis, A. E. (2007). Rapid evolution of flowering time by an annual plant in response to a climate fluctuation. *Proceedings of the National Academy of Sciences of the United States of America*, *104*(4), 1278–1282.

Fu, Y.-B., Peterson, G. W., Horbach, C., Konkin, D. J., Beiles, A., & Nevo, E. (2019). Elevated mutation and selection in wild emmer wheat in response to 28 years of global warming. *Proceedings of the National Academy of Sciences of the United States of America*, *116*(40), 20002–20008.

Golenberg, E. M. (1987). Estimation of gene flow and genetic neighborhood size by indirect methods in a selfing annual, *Triticum dicoccoides*. *Evolution; International Journal of Organic Evolution*, *41*(6), 1326–1334.

Golenberg, E. M. (1988). Outcrossing rates and their relationship to phenology in *Triticum dicoccoides*. *TAG. Theoretical and Applied Genetics*, *75*(6), 937–944.

Goudet, J. (2005). Hierfstat, a package for R to compute and test hierarchical F-statistics. *Molecular Ecology Notes*, *5*(1), 184–186.

Guénard, G., & Legendre, P. (2022). Hierarchical clustering with contiguity constraint in R. *Journal of Statistical Software*, *103*(7), 1–26.

Hendrick, M. F., Finseth, F. R., Mathiasson, M. E., Palmer, K. A., Broder, E. M., Breigenzer, P., & Fishman, L. (2016). The genetics of extreme microgeographic adaptation: An integrated approach identifies a major gene underlying leaf trichome divergence in Yellowstone *Mimulus guttatus*. *Molecular Ecology*, *25*(22), 5647–5662.

Horovitz, A. (1998). The soil seed bank in wild emmer. In N. Zencirci, Z. Kaya, Y. Anikster, & T. Adams (Eds.), *The proceedings of international symposium of in situ conservation of plant genetic diversity* (pp. 185–188). CRIFC.

Horovitz, A., & Feldman, M. (1991). Evaluation of the wild-wheat study at Ammiad. *Israel Journal of Botany*, *40*, 501–508.

Jombart, T., & Ahmed, I. (2011). Adegenet 1.3-1: New tools for the analysis of genome-wide SNP data. *Bioinformatics*, *27*(21), 3070–3071.

Keeling, C. D., Piper, S. C., Bacastow, R. B., Wahlen, M., Whorf, T. P., Heimann, M., & Meijer, H. A. (2001). Exchanges of atmospheric CO2 and 13CO2 with the terrestrial biosphere and oceans from 1978 to 2000. In *I. Global aspects, SIO reference series, scripps in (01-06)* (p. 88). Scripps Institution of Oceanography.

Kelly, J. K. (2022). The genomic scale of fluctuating selection in a natural plant population. *Evolution Letters*, *6*(6), 506–521.

Khoury, C. K., Carver, D., Greene, S. L., Williams, K. A., Achicanoy, H. A., Schori, M., León, B., Wiersema, J. H., & Frances, A. (2021). Crop wild relatives of the United States require urgent conservation action. *Proceedings of the National Academy of Sciences of the United States of America*, *117*(52), 33351–33357.

Kolis, K. M., Berg, C. S., Nelson, T. C., & Fishman, L. (2022). Population genomic consequences of life-history and mating system adaptation to a geothermal soil mosaic in yellow monkeyflowers. *Evolution; International Journal of Organic Evolution*, *76*(4), 765–781.

Legendre, P., Fortin, M. J., & Borcard, D. (2015). Should the mantel test be used in spatial analysis? *Methods in Ecology and Evolution/British Ecological Society*, *6*(11), 1239–1247.

Levy, A. A., & Feldman, M. (1988). Ecogeographical distribution of HMW glutenin alleles in populations of the wild tetraploid wheat Triticum turgidum var. dicoccoides. *TAG. Theoretical and Applied Genetics*, *75*(4), 651–658.

Levy, A. A., & Feldman, M. (2022). Evolution and origin of bread wheat. *The Plant Cell*, *34*, 2549–2567. https://doi.org/10.1093/PLCELL/KOAC130

Li, H. (2013). *Aligning sequence reads, clone sequences and assembly contigs with BWA-MEM*. http://arxiv.org/abs/1303.3997

Li, H., Handsaker, B., Wysoker, A., Fennell, T., Ruan, J., Homer, N., Marth, G., Abecasis, G., Durbin, R., & 1000 Genome Project Data Processing Subgroup. (2009). The sequence alignment/map format and SAMtools. *Bioinformatics*, *25*(16), 2078–2079.

Li, Y.-C., Fahima, T., Krugman, T., Beiles, A., Röder, M. S., Korol, A. B., & Nevo, E. (2000). Parallel microgeographic patterns of genetic diversity and divergence revealed by allozyme, RAPD, and microsatellites in Triticum dicoccoides at Ammiad, Israel. *Conservation Genetics*, *1*(3), 191–207.

Li, Y. C., Fahima, T., Peng, J. H., Röder, M. S., Kirzhner, V. M., Beiles, A., Korol, A. B., & Nevo, E. (2000). Edaphic microsatellite DNA divergence in wild emmer wheat, *Triticum dicoccoides*, at a microsite: Tabigha, Israel. *TAG. Theoretical and Applied Genetics. Theoretische Und Angewandte Genetik*, *101*(7), 1029–1038.

Machado, H. E., Bergland, A. O., Taylor, R., Tilk, S., Behrman, E., Dyer, K., Fabian, D. K., Flatt, T., González, J., Karasov, T. L., Kim, B., Kozeretska, I., Lazzaro, B. P., Merritt, T. J., Pool, J. E., O'Brien, K., Rajpurohit, S., Roy, P. R., Schaeffer, S. W., … Petrov, D. A. (2021). Broad geographic sampling reveals the shared basis and environmental correlates of seasonal adaptation in *Drosophila*. *eLife*, *10*, e67577. https://doi.org/10.7554/eLife.67577

McCullagh, P., & Nelder, J. (1989). *Generalized linear models (2nd ed.)* (F. L. Boca Raton (ed.)). Chapman and Hall/CRC.

Monnahan, P. J., & Kelly, J. K. (2017). The genomic architecture of flowering time varies across space and time in Mimulus guttatus. *Genetics*, *206*(3), 1621–1635.

Noy-Meir, I., Agami, M., & Anikster, Y. (1991). Changes in the population density of wild emmer wheat (*Triticum turgidum* var. *dicoccoides*) in a mediterranean grassland. *Israel Journal of Botany*, *40*, 385–395.

Noy-Meir, I., Agami, M., Cohen, E., & Anikster, Y. (1991). Floristic and ecological differentiation of habitats within a wild wheat population at Ammiad. *Israel Journal of Botany*, *40*, 363–384.

Ozbek, O., Millet, E., Anikster, Y., Arslan, O., & Feldman, M. (2007). Spatio-temporal genetic variation in populations of wild emmer wheat, *Triticum turgidum* ssp. *dicoccoides*, as revealed by AFLP analysis. *TAG. Theoretical and Applied Genetics. Theoretische Und Angewandte Genetik*, *115*(1), 19–26.

Paradis, E. (2010). Pegas: An R package for population genetics with an integrated-modular approach. *Bioinformatics*, *26*(3), 419–420.

Pisupati, R., Reichardt, I., Seren, Ü., Korte, P., Nizhynska, V., Kerdaffrec, E., Uzunova, K., Rabanal, F. A., Filiault, D. L., & Nordborg, M. (2017). Verification of Arabidopsis stock collections using SNPmatch, a tool for genotyping high-plexed samples. *Scientific Data*, *4*(1), 170184.

Poland, J. A., Brown, P. J., Sorrells, M. E., & Jannink, J.-L. (2012). Development of high-density genetic maps for barley and wheat using a novel two-enzyme genotyping-by-sequencing approach. *PLoS One*, *7*(2), e32253.

Poplin, R., Ruano-Rubio, V., DePristo, M. A., Fennell, T. J., Carneiro, M. O., der Auwera, G. A. V., Kling, D. E., Gauthier, L. D., Levy-Moonshine, A., Roazen, D., Shakir, K., Thibault, J., Chandran, S., Whelan, C., Lek, M., Gabriel, S., Daly, M. J., Neale, B., MacArthur, D. G., & Banks, E. (2018). Scaling accurate genetic variant discovery to tens of thousands of samples. *bioRxiv*, 201178. https://doi.org/10.1101/201178

Revell, L. J. (2012). Phytools: An R package for phylogenetic comparative biology (and other things). *Methods in Ecology and Evolution/British Ecological Society*, *3*(2), 217–223.

Rudman, S. M., Greenblum, S. I., Rajpurohit, S., Betancourt, N. J., Hanna, J., Tilk, S., Yokoyama, T., Petrov, D. A., & Schmidt, P. (2022). Direct observation of adaptive tracking on ecological time scales in drosophila. *Science*, *375*(6586), eabj7484.

Schemske, D. W. (1984). Population structure and local selection in *Impatiens pallida* (balsaminaceae), a selfing annual. *Evolution; International Journal of Organic Evolution*, *38*(4), 817–832.

Siepielski, A. M., Dibattista, J. D., & Carlson, S. M. (2009). It's about time: The temporal dynamics of phenotypic selection in the wild. *Ecology Letters*, *12*(11), 1261–1276.

Stoffel, M. A., Johnston, S. E., Pilkington, J. G., & Pemberton, J. M. (2021). Genetic architecture and lifetime dynamics of inbreeding depression in a wild mammal. *Nature Communications*, *12*(1), 1–10.

The 1001 Genomes Consortium. (2016). 1,135 genomes reveal the global pattern of polymorphism in *Arabidopsis thaliana*. *Cell*, *166*(2), 481–491.

Todesco, M., Owens, G. L., Bercovich, N., Légaré, J. S., Soudi, S., Burge, D. O., Huang, K., Ostevik, K. L., Drummond, E. B. M., Imerovski, I., Lande, K., Pascual-Robles, M. A., Nanavati, M., Jahani, M., Cheung, W., Staton, S. E., Muños, S., Nielsen, R., Donovan, L. A., … Rieseberg, L. H. (2020). Massive haplotypes underlie ecotypic differentiation in sunflowers. *Nature*, *584*(7822), 602–607.

Troth, A., Puzey, J. R., Kim, R. S., Willis, J. H., & Kelly, J. K. (2018). Selective trade-offs maintain alleles underpinning complex trait variation in plants. *Science*, *361*(6401), 475–478.

Venables, W. N., & Ripley, B. D. (2002). *Modern applied statistics with S*. Springer.

Volis, S., Anikster, Y., Olsvig-Whittaker, L., & Mendlinger, S. (2004). The influence of space in genetic-environmental relationships when environmental heterogeneity and seed dispersal occur at similar scale. *The American Naturalist*, *163*(2), 312–327.

Volis, S., Ormanbekova, D., & Shulgina, I. (2016). Fine-scale spatial genetic structure in predominantly selfing plants with limited seed dispersal: A rule or exception? *Plant Diversity*, *38*(2), 59–64.

Volis, S., Ormanbekova, D., Yermekbayev, K., Song, M., & Shulgina, I. (2015). Multi-approaches analysis reveals local adaptation in the emmer wheat (*Triticum dicoccoides*) at macro- but not microgeographical scale. *PLoS One*, *10*(3), e0121153.

Wintle, B. A., Kujala, H., Whitehead, A., Cameron, A., Veloz, S., Kukkala, A., Moilanen, A., Gordon, A., Lentini, P. E., Cadenhead, N. C. R., & Bekessy, S. A. (2019). Global synthesis of conservation studies reveals the importance of small habitat patches for biodiversity. *Proceedings of the National Academy of Sciences of the United States of America*, *116*(3), 909–914.

Wittmann, M. J., Bergland, A. O., Feldman, M. W., Schmidt, P. S., & Petrov, D. A. (2017). Seasonally fluctuating selection can maintain polymorphism at many loci via segregation lift. *Proceedings of the National Academy of Sciences of the United States of America*, *114*(46), E9932–E9941.

Wright, S. (1969). *Evolution and the genetics of populations. Vol. 2: The theory of gene frequencies*. University of Chicago Press.

Zheng, X., Levine, D., Shen, J., Gogarten, S. M., Laurie, C., & Weir, B. S. (2012). A high-performance computing toolset for relatedness and principal component analysis of SNP data. *Bioinformatics*, *28*(24), 3326–3328.

Zhu, T., Wang, L., Rodriguez, J. C., Deal, K. R., Avni, R., Distelfeld, A., McGuire, P. E., Dvorak, J., & Luo, M.-C. (2019). Improved genome sequence of wild emmer wheat Zavitan with the aid of optical maps. *G3*, *9*(3), 619–624.

Zsögön, A., Peres, L. E. P., Xiao, Y., Yan, J., & Fernie, A. R. (2021). Enhancing crop diversity for food security in the face of climate uncertainty. *The Plant Journal: For Cell and Molecular Biology*, *109*(2), 402–414.

SUPPORTING INFORMATION

Additional supporting information can be found online in the Supporting Information section at the end of this article.

How to cite this article: Dahan-Meir, T., Ellis, T. J., Mafessoni, F., Sela, H., Rudich, O., Manisterski, J., Avivi-Ragolsky, N., Raz, A., Feldman, M., Anikster, Y., Nordborg, M., & Levy, A. A. (2024). 36-year study reveals stability of a wild wheat population across microhabitats. *Molecular Ecology*, *00*, e17512. https://doi.org/10.1111/mec.17512